Quantitative Analysis of Severe Acute Respiratory Syndrome (SARS)-associated Coronavirus-infected Cells Using Proteomic Approaches

IMPLICATIONS FOR CELLULAR RESPONSES TO VIRUS INFECTION*[S]

Xiao-Sheng Jiang‡, Liu-Ya Tang‡, Jie Dai‡, Hu Zhou‡, Su-Jun Li‡, Qi-Chang Xia‡, Jia-Rui Wu‡§¶, and Rong Zeng‡‖

We present the first proteomic analysis on the cellular response to severe acute respiratory syndrome-associated coronavirus (SARS-CoV) infection. The differential proteomes of Vero E6 cells with and without infection of the SARS-CoV were resolved and quantitated with two-dimensional differential gel electrophoresis followed by ESI-MS/MS identification. Moreover isotope-coded affinity tag technology coupled with two-dimensional LC-MS/MS were also applied to the differential proteins of infected cells. By combining these two complementary strategies, 355 unique proteins were identified and quantitated with 186 of them differentially expressed (at least 1.5-fold quantitative alteration) between infected and uninfected Vero E6 cells. The implication for cellular responses to virus infection was analyzed in depth according to the proteomic results. Thus, the present work provides large scale protein-related information to investigate the mechanism of SARS-CoV infection and pathogenesis.   *Molecular & Cellular Proteomics 4:902–913, 2005.*

A new type of coronavirus was reported as the causal agent of severe acute respiratory syndrome (SARS)[1] in April 2003, and the genome of the SARS-CoV was sequenced by several groups (1–3). The properties of the SARS-CoV genome was analyzed in depth by bioinformatic tools (4, 5). In addition,

[1] The abbreviations used are: SARS, severe acute respiratory syndrome; SARS-CoV, SARS-associated coronavirus; 2D, two-dimensional; DIGE, differential gel electrophoresis; hnRNP, heterogeneous nuclear ribonucleoprotein; 2DE, two-dimensional electrophoresis; Cy, cyanine; DMEM, Dulbecco's modified Eagle's medium; FBS, fetal bovine serum; RP, reverse phase; MHV, mouse hepatitis virus; EF, elongation factor; eIF, eukaryotic initiation factor.

several important works on the proteins of SARS-CoV have been reported recently, including the identification of SARS-CoV 3C-like protease structure (6) and the identification of angiotensin-converting enzyme 2 as a functional receptor for the spike protein (7). In our recent work, we identified all of the predicted SARS-CoV structural proteins, nucleocapsid (N), membrane (M), spike (S), and envelope (E), using proteomic approaches and found a novel protein, SARS-CoV 3a (8, 9).

To uncover the mechanisms of cellular responses to the virus infection and identify potential drug targets of antiviral treatment, it is very useful to study the molecular profiling of virus-infected cells with high throughput and quantitative approaches. Analysis of gene expression profiles during viral infection is one of the powerful approaches to probe potential cellular genes involved in viral infection and pathogenesis (10). The recent development of proteomic analytic technology such as differential gel electrophoresis (DIGE) (11, 12) and ICAT (13, 14) also provides new tools for such studies.

As a method based on two-dimensional (2D) electrophoresis, DIGE allows two or three independent samples labeled with different fluorescent dyes such as cyanine-2 (Cy2), cyanine-3 (Cy3), and cyanine-5 (Cy5) to be run in one gel simultaneously and viewed individually using the different fluorescent properties of Cy2, Cy3, and Cy5, circumventing some of the reproducibility problems associated with 2D electrophoresis and providing more accurate quantitative information compared with other staining methods such as silver staining with the dynamic range over 3–4 orders of magnitude (11, 12). More recently, the combination of stable ICAT, LC, and MS/MS has emerged as an alternative gel-free quantitative proteomic technology (13, 14). In ICAT analysis, two pools of proteins are labeled respectively with isotopically light and heavy ICAT regents, which are chemically identical and therefore serve as a good internal standard for accurate quantification. Although LC-MS provides quantitative information based upon the relative abundances of the heavy and light peptides, LC-MS/MS provides qualitative information based upon the peptide molecular mass and amino acid sequence information. These two technologies have been proved to be

complementary for a comprehensive comparative proteomic analysis (15, 16). ICAT analysis showed a clear bias for proteins with high molecular mass, whereas the 2D electrophoresis or DIGE method could separate proteins in certain low molecular mass ranges and also identified cysteine-free proteins that were transparent to the ICAT analysis. Moreover ICAT analysis quantifies the sum of the protein species of one gene product, whereas the 2D electrophoresis or DIGE method quantifies at the level of resolved protein species, including post-translationally modified and processed polypeptides.

In the present work, systematic analyses of the proteome of SARS-CoV-infected cells were performed using 2D-DIGE followed by electrospray mass spectrometry identification and ICAT technology coupled with 2D-LC-MS/MS. Using these two complementary methods, the differentially expressed proteome profiles between Vero E6 cells with and without virus infection were created, and a total of 355 proteins or protein spots were identified and quantitated. Further analysis of these data provides the clues for understanding the infection and pathogenesis of the SARS-CoV and the virus-host interactions.

EXPERIMENTAL PROCEDURES

Materials—Analytical reagent grade chemicals were used throughout unless otherwise stated. Water was prepared using a Milli-Q water purification system (Millipore, Bedford, MA). Chemicals used for gel electrophoresis were purchased from Bio-Rad. Cy2, Cy3, Cy5, Precast IPG dry strips, pH 3–10 non-linear, and ECL PLUS Western blotting detection regents were purchased from Amersham Biosciences. Formic acid and guanidine hydrochloride were obtained from Sigma. HPLC grade ACN was from Fisher. Sequencing grade trypsin was obtained from Promega (Southampton, UK).

Cell Culture, Virus Infection, and Sample Preparation—African green monkey kidney cells (Vero E6, ATCC) were maintained in Dulbecco's modified Eagle's medium (DMEM; Invitrogen) supplemented with 10% fetal bovine serum (FBS; Invitrogen) at 37 °C in 5% CO_2.

For virus infection, Vero E6 cells were treated with the DMEM (2% FBS) containing SARS-CoV virions (BJ-01 isolate, provided by Academy of Military Medical Sciences) for 1 h. The virus medium was removed after the infection, and the infected cells were cultured in DMEM with 2% FBS at 37 °C in 5% CO_2. 24 h postinfection, the cells were washed with PBS twice and then lysed with a lysis buffer containing 40 mM Tris base, 60 mM DTT, 8 M urea, 4% CHAPS. The mixture was centrifuged in a microcentrifuge for 5 min, and the supernatant was collected as the infected cellular sample. All the experiments using the virus were carried on in a biosafety Level 3 laboratory.

DIGE—For DIGE analysis, cellular samples were precipitated overnight with 5 volumes of 50:50:0.1 volumes of ethanol:acetone:acetic acid at −20 °C and resolubilized in the lysis buffer (7 M urea, 2 M thiourea, 30 mM Tris-Cl, 4% CHAPS). The cell lysates (E6 or E6-V) were labeled with *N*-hydroxysuccinimidyl ester derivatives of the cyanine dyes Cy2, Cy3, and Cy5 (Amersham Biosciences) according to the manufacturer's guidelines. Typically 50 μg of lysate were minimally labeled with 400 pmol of Cy2, Cy3, or Cy5, respectively. Differentially labeled samples were mixed (Cy2-labeled standard, Cy3-labeled E6, and Cy5-labeled E6-V for one gel; Cy2-labeled standard, Cy5-labeled E6, and Cy3-labeled E6-V for another gel). An equal volume of 2× 2D sample buffer (7 M urea, 2 M thiourea, 4% CHAPS, 2% DTT, and 2% IPG buffer, pH 3–10 non-linear) was added to

provide 65 mM DTT to reduce the labeled samples for 15 min at room temperature. Then the samples were subjected to 2D-PAGE in the dark. The DIGE gels were scanned using Typhoon Variable Model Imagels 9400 (Amersham Biosciences). DeCyder (Amersham Biosciences) software was used for image analysis.

In-gel Trypsin Digestion—Changes observed in 2D-DIGE images were aligned with Phastgel Blue R-stained protein patterns in preparative gels. Spots of interest were cut manually. Gel pieces were digested as described by Yu *et al.* (17).

RP-HPLC-ESI-MS/MS Analysis—RP-HPLC was performed using a surveyor LC system (Thermo Finnigan, San Jose, CA) on a C_{18} column (RP, 180 μm × 150 mm, BioBasic® C_{18}, 5 μm, Thermo Hypersil-Keystone). The pump flow rate was split 1:120 to achieve a column flow rate of 1.5 μl/min. Mobile phase A was 0.1% formic acid in water, and mobile phase B was 0.1% formic acid in acetonitrile. The tryptic peptide mixtures were eluted using a gradient of 2–98% B over 60 min.

The mass spectral data shown here were acquired on an LTQ linear ion trap mass spectrometer (Thermo Finnigan) equipped with an electrospray interface operated in positive ion mode. The temperature of the heated capillary was set at 170 °C. A voltage of 3.4 kV applied to the ESI needle resulted in a distinct signal. Normalized collision energy was 35.0. The mass spectrometer was set so that one full MS scan was followed by three MS/MS scans on the three most intense ions from the MS spectrum with the following Dynamic Exclusion™ settings: repeat count, 2; repeat duration, 0.5 min; exclusion duration, 2.0 min.

ICAT Analysis—ICAT analysis was performed using the Cleavable ICAT™ reagent kit (Applied Biosystems, Foster City, CA) according to the manufacturer's guidelines with some modifications. For ICAT analysis, the cellular samples were precipitated and resolubilized in denaturing buffer (6 M guanidine hydrochloride, 100 mM Tris-Cl, pH 8.3). 100 μg of the E6 or E6-V protein sample in 80 μl of denaturing buffer were reduced at 37 °C for 2 h with 5 mM tributylphosphine (Bio-Rad) and alkylated at 37 °C for 2 h in the dark with ICAT-light and ICAT-heavy reagent, respectively. The samples were digested with trypsin at 37 °C for 20 h. Then the ICAT-labeled peptides were purified using the kit of ICAT™ Avidin Buffer Pack and Avidin Affinity Cartridge (Applied Biosystems) according to the manufacturer's guidelines.

2D LC-MS/MS—Orthogonal 2D LC-MS/MS was performed using a ProteomeX work station (Thermo Finnigan). The system was fitted with a strong cation exchange column (320-μm inner diameter × 100 mm, DEV SCX, Thermo Hypersil-Keystone) and two C_{18} RP columns (180 μm × 100 mm, BioBasic C_{18}, 5 μm, Thermo Hypersil-Keystone). The salt steps used were 0, 25, 50, 75, 100, 150, 200, 400, and 800 mM NH_4Cl synchronized with nine 140-min RP gradients. RP solvents were 0.1% formic acid in either water (A) or acetonitrile (B). The setting of the LCQ Deca Xplus ion trap mass spectrometer is as follows. One full MS scan was followed by three MS/MS scans on the three most intense ions from the MS spectrum according to the following Dynamic Exclusion settings: repeat count, 1; repeat duration, 0.5 min; exclusion duration, 3.0 min.

Data Base Searching—The acquired MS/MS spectra were automatically searched against the nonredundant human protein data base (NCBI (www.ncbi.nlm.nih.gov), December 4, 2003 release) using the TurboSEQUEST program in the BioWorks™ 3.1 software suite. For protein spot identification, an accepted SEQUEST result had to have a ΔCn score of at least 0.1 (regardless of charge state). Peptides with a +1 charge state were accepted if they were fully tryptic and had a cross correlation (Xcorr) of at least 1.8. Peptides with a +2 charge state were accepted if they had an Xcorr >2.5. Peptides with a +3 charge state were accepted if they had an Xcorr >3.7. For ICAT analysis, protein identification and quantification were achieved by using SEQUEST and EXPRESS software tools. Peptides with a +1

FIG. 1. **Cy dye image of the SARS-CoV-infected Vero E6 (*red*, Cy3-labeled) cells and uninfected Vero E6 cells (*green*, Cy5-labeled).** The image shown is of a 100-μg sample (50 μg each of Cy3- and Cy5-labeled lysates) run on a pH 3–10 non-linear gradient IPG strip and 12.5% polyacrylamide gel. The *red* or *green spots* indicate the differentially expressed proteins. The *spots circled* and *marked with numbers* have been identified and listed in Supplemental Table I.
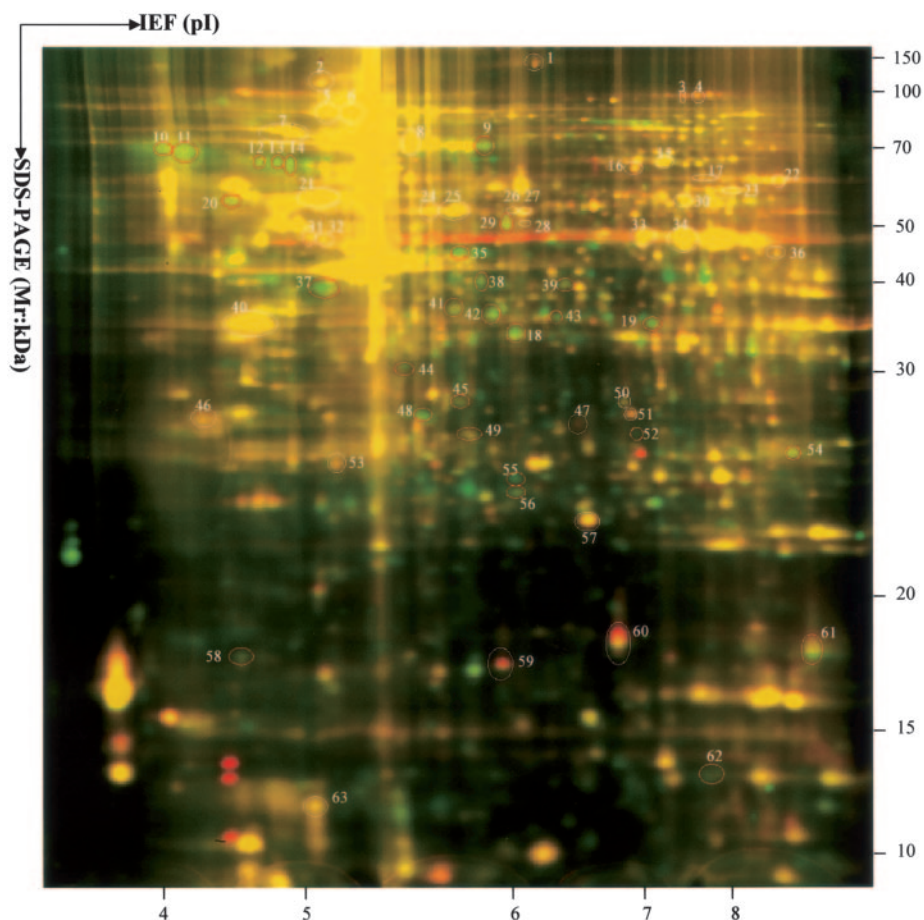
TABLE I

The number of differentially expressed proteins in SARS-CoV-infected or uninfected Vero E6 cells identified by DIGE and ICAT analysis

Ratio of E6:E6-V	≤0.50	≤0.67	≤ 0.83	0.83–1.20	≥1.20	≥1.50	≥2.00	Total
DIGE (unique proteins/protein spots)	11/14	17/21	23/28	0/0	27/35	13/15	3/3	48/63
ICAT (unique proteins)	37	48	69	48	205	119	51	322
Total (unique proteins)	46	60	86	48	221	126	52	355

charge state were accepted if they were fully tryptic and had an Xcorr of at least 1.5. Peptides with a +2 charge state were accepted if they had an Xcorr >2.0. Peptides with a +3 charge state were accepted if they had an Xcorr >2.5. Then the confirmation of protein identification and quantification of the peptides was further analyzed manually as described by Han *et al.* (14). Protein abundance ratios larger than +1.5 or smaller than −1.5 (or 0.67) were set as a threshold indicating significant changes (18).

Western Blotting—SDS-PAGE-separated proteins were transferred onto a nitrocellulose membrane (Protran, Schleicher & Schuell) on a Mini Trans-Blot Cell (Bio-Rad). The transferred membrane was blocked with 1× NET-Gelatin (150 mM NaCl, 5 mM EDTA, pH 8.8, 50 mM Tris-HCl, 0.05% Triton X-100, 8.3% gelatin) at room temperature for 1 h and then was incubated with corresponding primary antibodies (anti-HSP90 (rabbit), Santa Cruz Biotechnology, 1:5,000; anti-α-tubulin (mouse), Sigma, 1:600,000; anti-stathmin (rabbit), Calbiochem-Novabiochem, 1:5,000; anti-vimentin (mouse), Sigma, 1:1,000) for 1 h at room temperature, and then the membranes were incubated with the corresponding secondary antibodies. After being detected with ECL PLUS (Amersham Biosciences) according to the manufacturer's

instructions, the membrane was scanned using a Typhoon Scanner 9400 (Amersham Biosciences).

Bioinformatic Annotation—The theoretical pI and molecular mass values of proteins were defined by the program pepstats (www.hgmp.mrc.ac.uk/Software/EMBOSS). The protein function and subcellular location annotation was from the Swiss-Prot and TrEMBL protein data base (us.expasy.org/sprot/).

RESULTS

2D-DIGE Analysis of the SARS-CoV-infected and Uninfected Vero E6 cells—2D-DIGE as a qualitative and quantitative proteomic approach was performed to determine the differential proteomes of the SARS-CoV-infected and uninfected Vero E6 cells. The lysate from infected cells was labeled with Cy5, whereas the lysate from uninfected cells was labeled with Cy3. After electrophoresis and imaging, the Cy3 and Cy5 images were false colored in red and green, respectively, and two images were overlapped (Fig. 1). The biological

TABLE II

List of protein spots with at least 2.0-fold quantitative alteration in SARS-CoV-infected or uninfected Vero E6 cells based on DIGE analysis

VAMP, vesicle-associated membrane protein; PP2A, protein phosphatase 2A.

DIGE spot no.	Protein description	GI no.	Subcellular location	Theoretical MM (Da)/pI	Experimental MM (kDa)/pI	Peptide hits	Unique peptides	Sequence coverage	Ratio, DIGE (E6:E6-V)
								%	
Actin network protein									
42	Calponin, acidic isoform	gi|6225157|	Cytoskeletal	36,413.61/5.69	36.5/5.77	12	8	27.05	1:0.38
Chromosome-associated protein									
20	Chromatin assembly factor 1 subunit C	gi|1172846|	Nuclear	47,655.74/4.74	55.2/4.71	4	4	13.18	1:0.34
Cytoskeletal protein									
21	α-Tubulin 2	gi|20455316|	Cytoskeletal	50,151.71/4.94	55.4/5.20	15	12	39.69	1:2.00
Metabolic enzyme protein									
18	Pyruvate kinase, M1 isozyme	gi|20178296|	No annotation	57,913.83/7.96	34.3/5.89	25	10	19.21	1:0.37
19	Pyruvate kinase, M1 isozyme	gi|20178296|	No annotation	57,913.83/7.96	34.6/7.63	18	10	20.72	1:0.38
38	Galactokinase	gi|1730187|	No annotation	42,272.43/6.04	38.9/5.76	11	6	13.78	1:0.32
43	Transaldolase	gi|6648092|	Cytoplasmic	37,540.16/6.36	36.0/6.34	5	4	13.35	1:0.40
44	Pyruvate dehydrogenase E1 component β subunit	gi|129070|	Mitochondrial	39,219.39/6.20	31.4/5.43	18	9	29.25	1:0.49
Heterogeneous nuclear ribonucleoprotein									
32	hnRNP F	gi|1710628|	Nuclear	45,671.98/5.38	47.6/5.22	16	10	33.01	1:2.28
Intracellular trafficking protein									
12	Transmembrane protein (63 kDa)	gi|19920317|	Membrane	66,022.66/5.63	62.0/4.76	7	7	15.61	1:0.27
13	Transmembrane protein (63 kDa)	gi|19920317|	Membrane	66,022.66/5.63	61.7/4.78	5	4	10.30	1:0.34
52	VAMP-associated protein B/C	gi|24638339|	Membrane	27,228.36/6.85	27.3/7.49	5	5	21.81	1:0.49
Protein processing protein									
29	Mitochondrial processing peptidase β subunit	gi|29840827|	Membrane	54,366.18/6.38	48.4/5.84	9	5	11.86	1:0.40
Signaling protein									
14	PP2A subunit A, PR65-α isoform	gi|231443|	No annotation	65,223.6/4.96	59.8/4.89	7	6	11.04	1:0.31
47	14-3-3 protein τ	gi|112690|	Cytoplasmic	27,764.29/4.68	27.5/6.52	3	2	8.98	1:2.51
48	Annexin IV	gi|1703319|	No annotation	35,882.74/5.84	28.0/5.47	9	6	20.06	1:0.27
55	Growth factor receptor-bound protein 2	gi|121603|	No annotation	25,206.38/5.89	25.2/5.90	11	8	31.80	1:0.28

variation analysis mode of DeCyder was used for comparing the overlay image. The standardization was done by the comparison of normalized Cy3 and Cy5 protein spot volumes with the corresponding Cy2 standard spot volumes within each gel. Protein spots with an average ratio value greater than 1.2-fold and a t test p value <0.05 were selected for mass spectrometric identification. A total of 63 proteins belonging to 48 unique gene products were identified with ESI-LC-MS/MS (Supplemental Table I). Among those proteins, 17 proteins (21 protein spots) were down-regulated, whereas 13 proteins (15 protein spots) were up-regulated by at least 1.5-fold in SARS-CoV-infected cells (Table I). The identified protein spots with at least a 2.0-fold quantitative alteration in SARS-CoV-infected Vero E6 cells are listed in Table II. The

differentially expressed proteins are involved in various functions including cytoskeleton, actin-associated network, metabolic enzymes, and signal transduction (Table II and Supplemental Table I).

ICAT Analysis of the SARS-CoV-infected and Uninfected Vero E6 Cells—Recently a new proteomic approach, ICAT, has been developed to quantitatively analyze the protein differential expression, which is faster than the gel method. In the present work, the ICAT method coupled to 2D-LC-MS/MS was used for quantitative comparison of differential proteome profiles between SARS-CoV-infected cells and uninfected cells. Cysteines were labeled with light (^{12}C) and heavy (^{13}C) ICAT reagent, and labeled peptides were affinity-purified using an avidin column. The resultant peptides were first frac-

TABLE III

Selected list of proteins in SARS-CoV-infected or uninfected Vero E6 cells based on ICAT analysis

L, light; H, heavy; MuSK, muscle-specific tyrosine kinase; NSF, *N*-ethylmaleimide-sensitive factor.

Protein description	GI no.	Subcellular location	Peptide hits	Unique peptides	Ratio, ICAT (L:H; E6:E6-V)	Peptide sequence (charge/Xcorr/ΔCn)[a]
Actin network protein						
Anillin, actin-binding protein	gi|31657094|	Cytoskeletal	1	1	1:0.25	R.FGERC*QEHSKESPAR.S (2+/2.05/0.20)
α-Actinin 3 (F-actin cross-linking protein)	gi|728751|	Cytoskeletal	1	1	1:0.38	K.C*QLEINFNTLQTK.L (2+/3.16/0.36)
Destrin (actin-depolymerizing factor)	gi|5802966|	Cytoskeletal	4	1	1:2.77	K.HEC*QANGPEDLNR.A (3+/3.34/0.37)
Channel or transporter protein						
Potassium channel-modulatory factor 1	gi|31543383|	No annotation	1	1	1:2.59	R.HEGVSC*DAC*LK.G5 (2+/2.90/0.43)
Potassium channel subfamily K member 15	gi|24636282|	Membrane	1	1	1:2.97	K.VFC*MFYALLGIPLTLVTFQSLGER.L (3+/2.52/0.11)
Sodium bicarbonate transporter 4 isoform a	gi|15042959|	No annotation	1	1	1:8.84	R.FFGGLC*LDIK.R (2+/2.19/0.20)
Chromosome-associated protein						
DEK protein	gi|544150|	Nuclear	1	1	1:12.45	K.C*PEILSDESSSDEDEKK.N (3+/2.90/0.20)
High mobility group protein 4	gi|20138144|	Nuclear	1	1	1:2.20	K.RPPSGFFLFC*SEFRPK.I (3+/3.70/0.34)
Condensin subunit 2	gi|30172801|	Cytoplasmic and nuclear	1	1	1:2.21	K.TAASFDEC*STAGVFLSTLHC*QDYR.S (3+/4.73/0.54)
Heat shock protein						
HSP 90-α	gi|123678|	Cytoplasmic	3	1	1:2.08	K.HGLEVIYMIELIDKYC*VQQLK.E (3+/3.58/0.11)
Stress-induced phosphoprotein 1	gi|400042|	No annotation	2	1	1:2.18	K.DC*EEC*IQLEPTFIK.G (2+/2.54/0.25)
Heterogeneous nuclear ribonucleoprotein[b]						
hnRNP D0	gi|13124489|	Nuclear	4	1	1:1.51	R.GFC*FITFK.E (2/2.27/0.41)
hnRNP U	gi|6226894|	Nuclear	4	1	1:1.77	K.TC*NC*ETEDYGEK.F (2+/2.68/0.37)
hnRNP core protein A1	gi|133254|	Nuclear	6	1	1:1.90	K.YHTVNGHNC*EVR.S (2+/3.58/0.24)
hnRNP I	gi|131528|	Nuclear	2	1	1:1.95	K.LSLDGQNIYNAC*C*TLR.I (2+/3.37/0.41)
hnRNP K isoform a	gi|14165437|	Cytoplasmic and nuclear	4	1	1:2.00	K.LFQEC*C*PHSTDR.V (2+/3.55/0.45)
hnRNP A0	gi|8134660|	Nuclear	1	1	1:2.04	R.GHFEAFGTLTDC*VVVVNPQTK.R (3+/2.98/0.43)
hnRNP D-like	gi|4885423|	No annotation	8	1	1:2.18	R.RGFC*FITYTDEEPVKK.L (3+/4.30/0.43)
hnRNP E2	gi|6707736|	Nuclear	1	1	1:2.27	R.INISEGNC*PER.I (2+/2.84/0.29)
Intracellular trafficking protein						
Translocation protein SEC63 homolog	gi|18203500|	Endoplasmic reticulum	1	1	1:0.50	R.APTLASLENCMKLSQMAV-QGLQQFK.S (3+/2.74/0.29)
Synaptophysin-like protein isoform a; pantophysin	gi|5803185|	Vesicular	1	1	1:2.28	K.GQTEIQVNC*PPAVTENKTVTATFGYPFR.L (3+/2.71/0.21)
α-Soluble NSF attachment protein	gi|6226705|	Membrane	1	1	1:9.51	K.C*LLKVAGYAALLEQYQK.A (3+/2.66/0.13)
Metabolic enzyme						
Vacuolar ATP synthase catalytic subunit A	gi|22096378|	Endoplasmic reticulum	1	1	1:0.36	R.FCPFYKTVGMLSNMIAFYDMARR.A (3+/3.26/0.21)
Pyruvate dehydrogenase E1 component α subunit	gi|129063|	Mitochondrial	1	1	1:0.36	K.LPCIFICENNR.Y (2+/2.13/0.23)
FK506-binding protein 4	gi|399866|	Cytoplasmic and nuclear	2	1	1:0.41	K.VGEVCHITCKPEYAYGSAGSPPK.I (3+/2.86/0.23)
Alanine-glyoxylate aminotransferase 2	gi|17432913|	Mitochondrial	1	1	1:0.45	K.CLQHFNTFGGNPMACAIGSAVLEVIK.E (3+/2.77/0.16)
GMP reductase 2	gi|25008511|	No annotation	1	1	1:2.10	K.GHIISDGGC*SC*PGDVAK.A (3+/2.63/0.16)
Succinyl-CoA synthetase, α chain	gi|20141765|	Mitochondrial	6	1	1:2.16	R.LIGPNC*PGVINPGEC*K.I (2+/3.78/0.52)
Thioredoxin-like protein p46	gi|29839560|	Endoplasmic reticulum	19	2	1:2.44 ± 0.45	K.VDC*TAHSDVC*SAQGVR.G (2+/4.18/0.50); K.VDC*TQHYELC*SGNQVR.G (3+/4.27/0.35)
UDP-glucose 6-dehydrogenase	gi|6175086|	No annotation	1	1	1:3.56	R.AVQALC*AVYEHWVPR.E (3+/2.60/0.30)
Protein degradation						
Ovochymase	gi|34419641|	No annotation	1	1	1:2.03	R.YLLDYRGRLEC*SWVLR.V (3+/2.62/0.17)
Proteasome subunit P50	gi|20532406|	Cytoplasmic and nuclear	3	1	1:2.22	R.C*TDDFNGAQC*K.A (2+/3.16/0.45)

TABLE III— *continued*

Protein description	GI no.	Subcellular location	Peptide hits	Unique peptides	Ratio, ICAT (L:H; E6:E6-V)	Peptide sequence (charge/Xcorr/ΔCn)[a]
Ribosomal protein[b]						
Ribosomal protein S4	gi|4506725|	Ribosomal	11	2	1:1.52 ± 0.33	K.LREC*LPLIIFLR.N (3+/3.82/0.32)
60 S ribosomal protein L10a	gi|15431288|	Ribosomal	6	1	1:1.58	K.FSVC*VLGDQQHC*DEAK.A (2+/2.97/0.37)
40 S ribosomal protein S15a	gi|14165469|	Ribosomal	1	1	1:1.61	K.C*GVISPR.F (2+/2.10/0.16)
40 S ribosomal protein S21	gi|4506699|	Ribosomal	2	1	1:1.65	K.TYAIC*GAIR.R (2+/2.27/0.25)
40 S ribosomal protein S26	gi|15011936|	Ribosomal	6	1	1:1.66	K.LHYCVSCAIHSK.V (3+/3.10/0.53)
40 S ribosomal protein S12	gi|14277700|	Ribosomal	9	2	1:1.66 ± 0.12	K.LVEALC*AEHQINLIK.V (2+/4.17/0.19); R.KVVGC*SC*VVVK.D (2+/2.72/0.21)
40 S ribosomal protein S11	gi|4506681|	Ribosomal	13	1	1:2.03	R.DVQIGDIVTVGEC*RPLSK.T (2+/4.65/0.53)
40 S ribosomal protein SA	gi|125969|	Ribosomal	4	1	1:2.06	R.ADHQPLTEASYVNLPTIALC*NTDSPLR.Y (3+/5.15/0.49)
40 S ribosomal protein S27a	gi|4506713|	Ribosomal	7	2	1:2.18 ± 0.23	K.C*C*LTYC*FNKPEDK.- (2+/3.35/0.40); R.EC*PSDEC*GAGVFMASHFDR.H (3+/4.17/0.45)
Signaling protein						
Cell division protein kinase 6	gi|266423|	No annotation	1	1	1:0.17	R.ADQQYECVAEIGEGAYGK.V (3+/2.51/0.13)
Ectodysplasin A receptor-associated adapter protein	gi|21362527|	Cytoplasmic	1	1	1:0.40	K.ENCTCSSCLLR.A (2+/2.25/0.15)
Transducin β chain 5	gi|38258891|	No annotation	1	1	1:0.45	R.YYPSGDAFASGSDDATCRLYDLR.A (3+/2.51/0.22)
Phosphoinositide-3-kinase, regulatory subunit 4, p150	gi|23943912|	No annotation	1	1	1:0.49	K.PVIPVLSSTILPSTYQIRITTC*K.T (3+/2.55/0.12)
Galectin-1	gi|126155|	No annotation	23	2	1:2.07 ± 0.35	K.DSNNLC*LHFNPR.F (2+/3.34/0.32); R.FNAHGDANTIVC*NSK.D (2+/4.70/0.59)
Receptor tyrosine kinase MuSK	gi|5031927|	No annotation	1	1	1:2.18	R.EYC*LAVKELFC*AKEWLVMEEK.T (3+/2.82/0.15)
Fibroblast growth factor-9	gi|544290|	Secreted	1	1	1:2.42	R.QLYCRTGFHLEIFPNGTIQGTR.K (3+/2.78/0.22)
Apoptotic chromatin condensation inducer in the nucleus	gi|7662238|	Nuclear	1	1	1:2.47	K.FLC*ADYAEQDELDYHR.G (3+/3.36/0.42)
Testin	gi|17380320|	No annotation	2	1	1:2.52	K.NHAVVC*QGC*HNAIDPEVQR.V (3+/3.03/0.37)
Tenascin X precursor	gi|9087217|	Secreted	1	1	1:3.68	R.VRGEESEVTVGGLEPGC*K.Y (3+/3.58/0.11)
Transcription or replication factor						
DNA ligase I	gi|118773|	Nuclear	1	1	1:0.38	K.GLFVACRHSEARFIAR.S (3+/2.65/0.22)
Cleavage- and polyadenylation-specific factor 6, 68-kDa subunit	gi|5901928|	Nuclear	1	1	1:2.01	K.RELHGQNPVVTPC*NK.Q (3+/2.69/0.40)
DNA helicase homolog	gi|5523990|	Nuclear	1	1	1:4.31	R.QQLPLQLAWAMSIHKSQGMTLDC*VEISL-GR.V (3+/3.08/0.12)
Translation factor[b]						
eIF-1	gi|1174483|	No annotation	8	2	1:1.56 ± 0.08	K.FAC*NGTVIEHPEYGEVIQLQGDQR.K (3+/4.16/0.38); K.NICQFLVEIGLAK.D (2+/2.20/0.15)
eIF-5	gi|27735202|	No annotation	1	1	1:1.60	K.FVLCPECENPETDLHVNPK.K (3+/2.93/0.27)
eIF-5A2 protein	gi|9966867|	No annotation	1	1	1:1.76	K.KYEDIC*PSTHNMDVPNIK.R (3+/3.42/0.41)
EF-Tu, mitochondrial precursor	gi|1706611|	Mitochondrial	4	1	1:2.17	R.HYAHTDC*PGHADYVK.N (3+/3.96/0.49)
Other function protein						
WD repeat domain 17 isoform 1	gi|31317311|	No annotation	1	1	1:0.42	R.IWDYTQDACINILNGHTAPVR.G (3+/2.52/0.15)
Ran-binding protein 2	gi|1709217|	Nuclear	3	1	1:2.03	K.C*IAC*QNPGK.Q (2+/2.86/0.43)
Hyaluronan-binding protein 4	gi|24307947|	No annotation	1	1	1:2.06	R.YGGNDKIAVRTEDNMGGC*GVR.T (3+/2.60/0.17)
Metallothionein II	gi|127397|	No annotation	1	1	1:2.51	K.CAQGCICK.G (2+/2.20/0.15)

[a] Select list of the peptides with the best assignment scores for protein identification and quantification by ICAT analysis. C/C*, ICAT light/heavy reagent-labeled cysteine-including peptide, respectively.

[b] For heterogeneous nuclear ribonucleoproteins, ribosomal proteins, and translation factors, proteins with at least 1.5-fold alteration are listed. The MS and MS/MS spectra for identification and quantitation of these proteins are shown in Supplemental Figs. 4–24.

tionated with nine salt steps, and each step was further separated using a reverse phase column and analyzed with ESI-MS/MS. The relative quantitation of proteins in infected and uninfected cells was determined from the relative abundance ratio of labeled peptides. By this approach, the relative abundance of 322 proteins was measured (Supplemental Table I). Individual peptide sequences and their probability scores for identification and quantitation of those proteins are listed in Supplemental Table II. Among these cellular proteins identified from the infected cells, 167 proteins had at least 1.5-fold quantitative alterations with 119 proteins up-regulated and 48 proteins down-regulated (Table I). Some selected proteins with quantitative alterations are listed in Table III. In addition, two SARS proteins, M and S, were observed to be significantly increased in the infected cells (data not shown).

Comparison and Validation of the Quantitation of Differential Proteins—We used 2D-DIGE and ICAT methods to investigate the differentially expressed proteins in Vero E6 cells infected with SARS-CoV. These two methods are both more sensitive and accurate than traditional methods such as silver staining (data not shown). We further used Western blot assay to confirm the differential expression of the proteomes identified by those two methods. The Western blotting results showed that the ratios of four representative proteins, α-tubulin, HSP90, OP18 stathmin, and vimentin, between the infected and uninfected cells were in agreement with those obtained from 2D-DIGE or ICAT approaches (Fig. 2 and Supplemental Figs. 1–3).

It was observed that the overall expression alterations were similar with both quantitative proteomic approaches, although only 15 differential proteins were identified by both 2D-DIGE and ICAT approaches (Table IV). In addition, the DIGE method detected more isoforms of proteins than the ICAT approach did (Table IV).

Subcellular Location and Function Classification of the Differential Proteins—In the present work, a total of 355 unique gene products of SARS-CoV-infected and uninfected cells were identified and quantitated with either the 2D-DIGE or ICAT method of which 186 proteins had at least 1.5-fold quantitative alterations (Table I and Supplemental Table I). Among those 186 differentially expressed proteins, 60 proteins were down-regulated in infected cells, whereas 126 proteins were up-regulated. These proteins were further classified according to their subcellular locations (Fig. 3). Interestingly, the up-regulated proteins in infected cells were mainly located in the nuclei (about 25%, see Fig. 3*A*), whereas down-regulated proteins distributed within the cells (Fig. 3*B*).

Those 186 proteins with at least 1.5-fold differential expression were further classified according to their functions (Supplemental Table I). Fig. 4 presents the functional categories of these proteins. In these identified SARS-CoV-infected cellular proteins, the enzymes, signal proteins, ribosomal proteins, and heterogeneous nuclear ribonucleoproteins (hnRNPs) consisted of about 45% of the total up-regulated proteins (Fig.
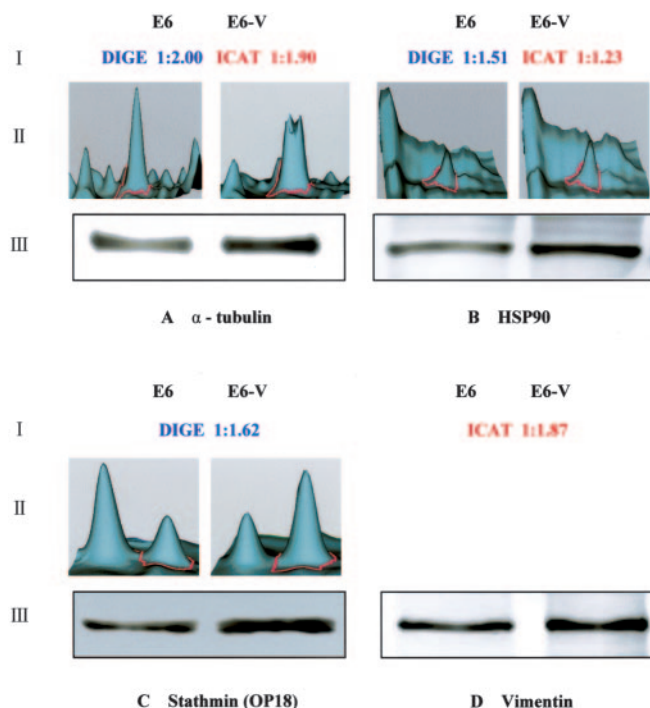

FIG. 2. **Protein quantitative confirmation with Western blotting.** *A*, α-tubulin; *B*, HSP90; *C*, OP18 stathmin; *D*, vimentin. *Row I* indicates the DIGE or ICAT analysis ratio. *Row II* shows the three-dimensional fluorescence intensity profiles of the individual spots. *Row III* shows the Western blot results. The MS and MS/MS spectra of ICAT analysis for proteins α-tubulin, HSP90, and vimentin are shown in Supplemental Figs. 1–3, respectively.

4*A*). On the other hand, more than half of the down-regulated proteins of the infected cells were involved in the enzymatic reactions, signal transduction, immune responses, and actin networks (Fig. 4*B*).

DISCUSSION

From the literature, very few studies have been performed to analyze the interaction between coronavirus and host cells with proteomic approaches. In the present work, we used two quantitative proteomic assays, DIGE and ICAT, to determine the differentially expressed protein profiles of SARS-CoV-infected and uninfected cells. It was noted that only a few proteins were identified by both DIGE and ICAT approaches, suggesting that these two methods are complementary to each other. In addition, the main difference of those two assays is that ICAT only determines the overall expression level, whereas DIGE can detect and quantitate protein isoforms in a gel. Although the DIGE method can detect protein isoforms possibly caused by post-translational modifications, it has limitations in identification of proteins with very high or low molecular weights, extreme acidic/alkaline proteins, and low abundance proteins. In our present work, 45 proteins that have a molecular mass greater than 100 kDa were identified among which only two proteins were detected by the DIGE approach. Moreover all 22 identified proteins with pI > 10

TABLE IV
List of the proteins or protein spots identified and quantitated in SARS-CoV-infected or uninfected Vero E6 cells by both ICAT and DIGE analysis

Protein description	GI no.	Subcellular location	Theoretical MM (Da)/pI	DIGE spot no.	Experimental MM (kDa)/pI	Peptide hits	Unique peptides	Sequence coverage	Ratio ICAT (L:H; E6:E6-V)	Ratio DIGE (E6:E6-V)
								%		
Actin network protein										
Cofilin, non-muscle isoform	gi|116848|	Cytoplasmic and nuclear	18,502.47/8.22	60	19.0/8.30	14	2	15.66	1:1.59 ± 0.08	
				61	19.1/6.82	1	1	8.43		1:1.81
						120	35	56.12		1:0.85
Chromosome-associated protein										
Chromatin assembly factor 1 subunit C	gi|1172846|	Nuclear	47,655.74/4.74			1	1	3.76	1:1.63	
				20	55.2/4.71	4	4	13.18		1:0.34
Cytoskeletal protein										
α-Tubulin 2	gi|20455316|	Cytoskeletal	49,959.62/4.98			2	2	8.22	1:1.90 ± 0.10	
				21	55.4/5.20	15	12	39.69		1:2.00
Heat shock protein										
HSP 90-β	gi|17865718|	Cytoplasmic	83,264.38/4.97			1	1	2.62	1:1.23	
				6	82.5/5.31	54	24	34.53		1:1.51
				5	82.9/5.27	20	14	26.80		1:1.32
Heat shock cognate 71-kDa protein	gi|123648|	No annotation	70,897.96/5.37			7	1	3.41	1:1.34	
				9	70.8/5.78	13	10	19.04		1:0.52
				11	70.4/4.18	15	11	21.05		1:0.54
				10	71.0/4.00	33	19	30.65		1:0.72
Hsc70-interacting protein	gi|6686278|	Cytoplasmic	41,331.83/5.18			3	1	4.61	1:1.41	
				31	48.0/4.99	13	7	15.99		1:1.73
Stress-induced phosphoprotein 1	gi|400042|	No annotation	62,639.39/6.40			2	1	2.58	1:2.18	
				15	63.4/7.35	81	30	46.78		1:1.22
Heterogeneous nuclear ribonucleoprotein										
hnRNP H	gi|1710632|	Nuclear	49,229.59/5.89			1	1	4.23	1:1.57	
				28	48.9/6.04	29	12	33.41		1:1.68
				27	51.0/5.83	19	11	34.97		1:1.60
				26	51.0/5.83	49	12	30.96		1:1.46
Metabolic enzyme protein										
Nucleoside diphosphate kinase B	gi|127983|	Cytoplasmic, and nuclear	17,298.03/8.52			1	1	5.92		1:1.05
				62	13.3/7.92	2	1	5.92		1:0.57
α enolase	gi|119339|	Cytoplasmic	47,168.91/7.01			19	3	11.98	1:1.48 ± 0.08	
				33	47.2/7.00	136	25	50.00		1:1.40
				34	47.4/7.67	188	20	46.08		1:1.25
Pyruvate kinase, M1 isozyme	gi|20178296|	No annotation	57,936.87/7.96			17	5	11.30	1:1.75 ± 0.44	
				22	57.5/8.21	120	35	56.12		1:1.42
				17	58.0/8.00	9	7	12.43		1:1.22
				18	34.3/5.89	25	10	19.21		1:0.37
				19	34.6/7.63	18	10	20.72		1:0.38
Thioredoxin	gi|135773|	No annotation	11,737.48/4.82			5	1	8.57	1:1.77	
				63	12.0/4.80	7	5	27.62		1:1.28
UDP-glucose 6-dehydrogenase	gi|6175086|	No annotation	55,024.12/6.73			1	1	3.04	1:3.56	
				23	56.6/8.08	14	13	29.35		1:1.27
Signaling protein										
14-3-3 protein τ	gi|112690|	Cytoplasmic	27,764.29/4.68			3	1	4.49	1:1.57	
				47	27.5/6.52	3	2	8.98		1:2.51
				46	27.8/4.60	2	1	5.71		1:1.29
Annexin IV	gi|1703319|	No annotation	35,882.74/5.84			5	2	7.52	1:1.62 ± 0.19	
				48	28.0/5.47	9	6	20.06		1:0.27

were contributed by the ICAT method (Supplemental Table I). Concerning the capacity of the protein identification, the DIGE approach identified 48 unique proteins, whereas the ICAT approach obtained 322 proteins; the ICAT approach especially identified more signal proteins, which usually are low abundance proteins in a cell.

Based on the identified proteins in the present work, we can gain an overall insight into the altered protein expression of the host cell responding to SARS-CoV infection. Among the differentially expressed host proteins, many of them participated in viral RNA replication and translation (Tables II and III and Supplemental Table I). It is known that positive-strand RNA viruses recruit normal components of host cellular RNA-processing or translation machineries for the viral RNA synthesis and protein synthesis (19, 20). Our data here indicate that SARS-CoV virus uses a similar strategy when infecting the host cells.
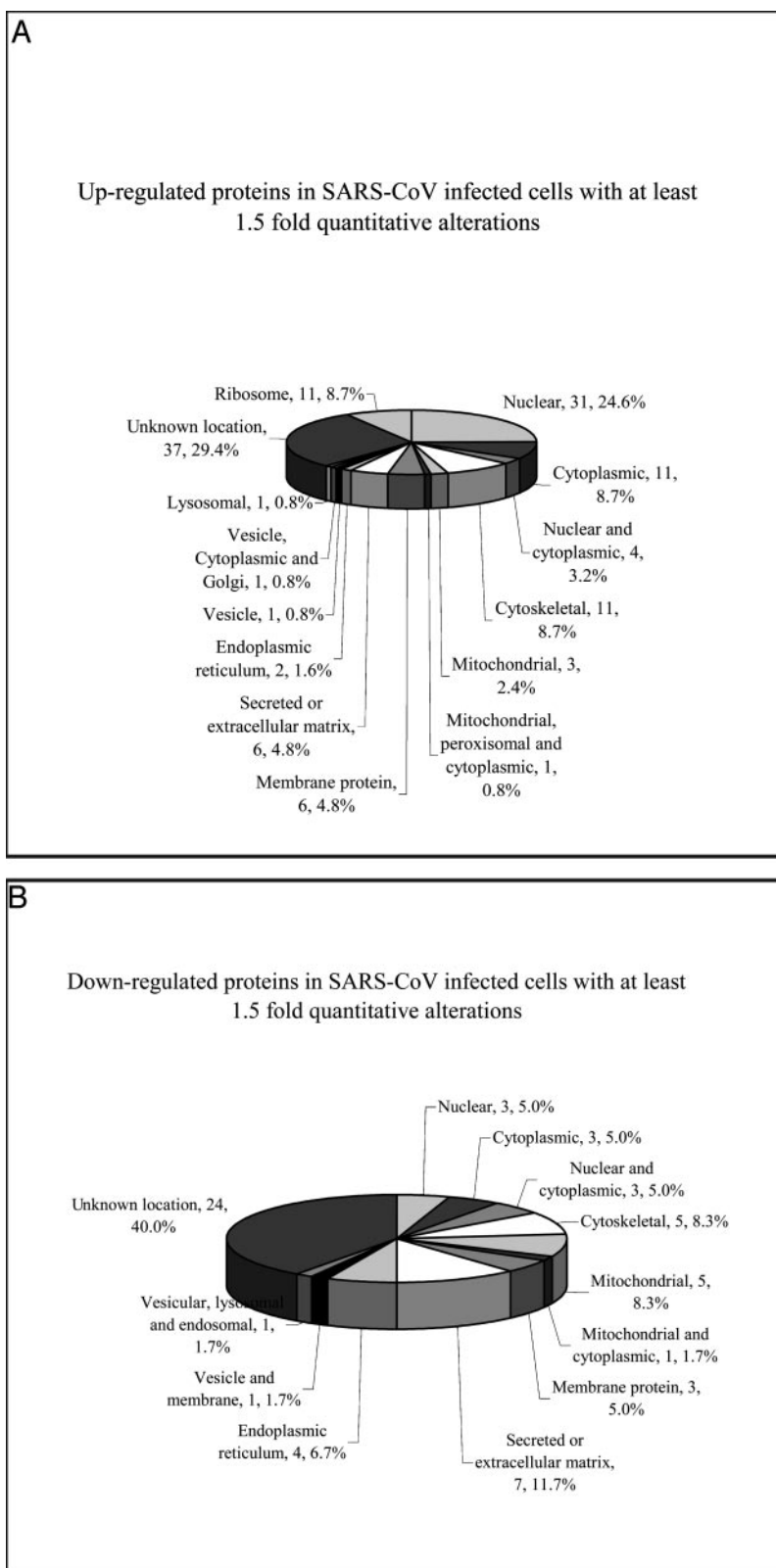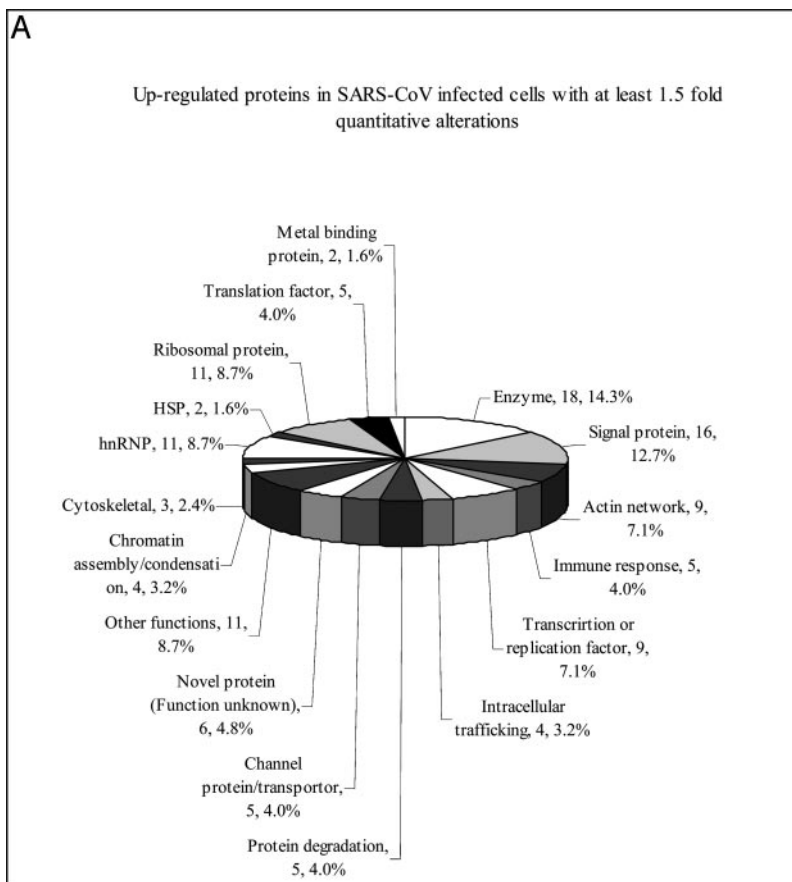
Fig. 3. **Subcellular location of the proteins with differential expression (≥1.5-fold alterations) in Vero E6 cells infected with SARS-CoV.** *A*, up-regulated proteins. *B*, down-regulated proteins.

hnRNPs are described as a major group of nuclear RNA-binding proteins that function in transcription, RNA processing, mRNA translation, and turnover (21, 22). In the present work, a total of eight kinds of hnRNP factors were identified to be up-regulated significantly in SARA-CoV-infected cells (Table III and Supplemental Figs. 4–11), suggesting that the virus

FIG. 4. **Functional classification of the proteins with differential expression (≥1.5-fold alteration) in Vero E6 cells infected with SARS-CoV.** *A*, up-regulated proteins. *B*, down-regulated proteins.
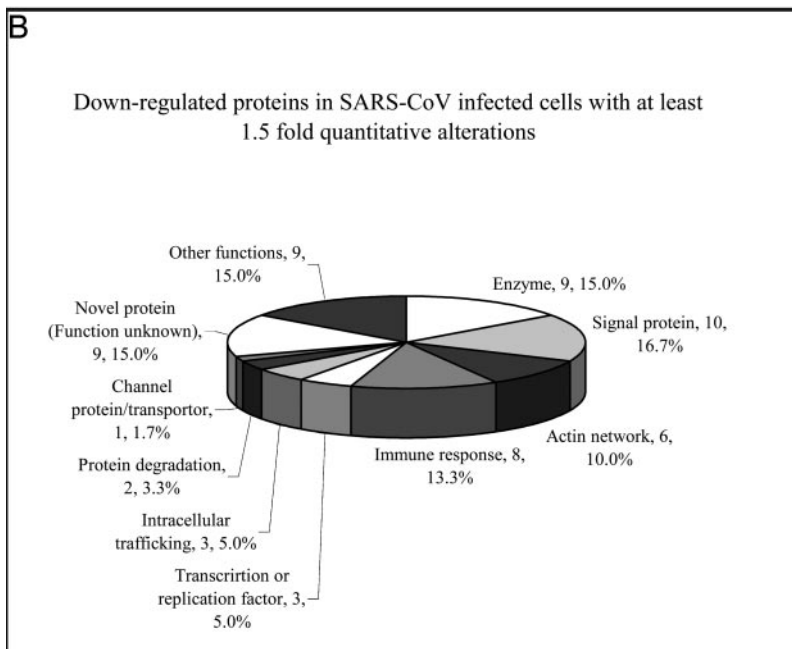
requires the function of hnRNPs. Among these identified hnRNPs, hnRNP A1, hnRNP K, and poly(rC)-binding protein have been reported previously to participate in positive-strand virus genome replication. Moreover, the rest of the hnRNPs were described here for the first time to be involved in coronavirus infection (Table III).

HnRNP A1 has been extensively studied for its role in viral RNA replication. Some reports showed that hnRNP A1 could

bind the RNA of a mouse coronavirus (mouse hepatitis virus (MHV)) at the 3′-end of both plus and minus strands and modulate MHV RNA synthesis (21–23). However, a recent work argued that hnRNP A1 might not be necessary for MHV viral genome replication or transcription *in vivo* because the absence of hnRNP A1 in infected cells had no effect on the production of infectious MHV (24). In addition, another experiment revealed that a mouse erythroleukemia cell line, CB3, did not express hnRNP A1 but still supported MHV replication, whereas hnRNP A2/B1, hnRNP A/B, and hnRNP A3 could replace hnRNP A1 in cellular functions and viral infection (25). In the present study, hnRNP A1 has been identified and quantitated by ICAT analysis based on doubly charged and both ICAT light reagent- and heavy reagent-labeled peptide K.YHTVNGHNCEVR.K, a typical trypsin-digested peptide fragmentized at the lysine or arginine carboxyl end, which is marked with the period (Supplemental Fig. 4) and shows up-regulated expression (E6:E6-V, 1:1.90) in SARS-CoV-infected cells (Table III). The present work provides a new explanation for such controversial results on hnRNP A1, *i.e.* several different hnRNP factors in the infected cells may form a functional hnRNP complex participating in viral RNA metabolism in which one hnRNP factor can be substituted by another without disruption of the function of the hnRNP complex.

The viral genomic RNA of all positive-strand RNA viruses need to be translated by recruited host factors (26, 27). A recent report showed that the decrease of 60 S ribosome protein levels reduced a positive-strand virus (Brome mosaic virus)-directed expression in yeast cells (27). The quantitatively proteomic approaches used here revealed that about nine kinds of ribosomal proteins, including components of both 40 and 60 S ribosomal subunits, were up-regulated significantly (Table III and Supplemental Figs. 12–20), suggesting that overall up-regulation of the ribosomal protein expression is required for positive-strand RNA virus propagation in host cells.

Translation factors have been well documented to participate in the processes of the virus RNA and protein synthesis (26, 28). For example, the elongation factors EF-Tu and EF-Ts were found to bind tightly to the viral RNA-dependent RNA polymerase (29). We also identified the up-regulation of EF-Tu expression in SARS-CoV-infected cells (Table III and Supplemental Fig. 21). Some studies showed that eukaryotic translation initiation factor eIF-4 protein complex is involved in viral protein synthesis (26). On the other hand, the present studies revealed that the expression of eIF-1, eIF-5, and eIF-5A2 was increased in the infected cells, suggesting that these factors play a role in the process of SARS-CoV viral translation (Table III and Supplemental Figs. 22–24).

In summary, we present the first quantitative proteomic work on the cellular responses to SARS-CoV infection, establishing so far the most comprehensive differential proteomic index for SARS-CoV-infected cells. The identified differential profile derived from the infected cellular proteins gives the implications for the infectivity and pathogenesis of SARS-CoV and provides a valuable resource for diagnosis, drug development, and clinical treatment for SARS.

REFERENCES

1. Ksiazek, T. G., Erdman, D., Goldsmith, C. S., Zaki, S. R., Peret, T., Emery, S., Tong, S., Urbani, C., Comer, J. A., Lim, W., Rollin, P. E., Dowell, S. F., Ling, A. E., Humphrey, C. D., Shieh, W. J., Guarner, J., Paddock, C. D., Rota, P., Fields, B., DeRisi, J., Yang, J. Y., Cox, N., Hughes, J. M., LeDuc, J. W., Bellini, W. J., Anderson, L. J., and SARS Working Group (2003) A novel coronavirus associated with severe acute respiratory syndrome. *N. Engl. J. Med.* **348,** 1953–1966

2. Marra, M. A., Jones, S. J., Astell, C. R., Holt, R. A., Brooks-Wilson, A., Butterfield, Y. S., Khattra, J., Asano, J. K., Barber, S. A., Chan, S. Y., Cloutier, A., Coughlin, S. M., Freeman, D., Girn, N., Griffith, O. L., Leach, S. R., Mayo, M., McDonald, H., Montgomery, S. B., Pandoh, P. K., Petrescu, A. S., Robertson, A. G., Schein, J. E., Siddiqui, A., Smailus, D. E., Stott, J. M., Yang, G. S., Plummer, F., Andonov, A., Artsob, H., Bastien, N., Bernard, K., Booth, T. F., Bowness, D., Czub, M., Drebot, M., Fernando, L., Flick, R., Garbutt, M., Gray, M., Grolla, A., Jones, S., Feldmann, H., Meyers, A., Kabani, A., Li, Y., Normand, S., Stroher, U., Tipples, G. A., Tyler, S., Vogrig, R., Ward, D., Watson, B., Brunham, R. C., Krajden, M., Petric, M., Skowronski, D. M., Upton, C., and Roper, R. L. (2003) The genome sequence of the SARS-associated coronavirus. *Science* **300,** 1399–1404

3. Ruan, Y. J., Wei, C. L., Ee, A. L., Vega, V. B., Thoreau, H., Su, S. T., Chia, J. M., Ng, P., Chiu, K. P., Lim, L., Zhang, T., Peng, C. K., Lin, E. O., Lee, N. M., Yee, S. L., Ng, L. F., Chee, R. E., Stanton, L. W., Long, P. M., and Liu, E. T. (2003) Comparative full-length genome sequence analysis of 14 SARS coronavirus isolates and common mutations associated with putative origins of infection. *Lancet* **361,** 1779–1785

4. Rota, P. A., Oberste, M. S., Monroe, S. S., Nix, W. A., Campagnoli, R., Icenogle, J. P., Penaranda, S., Bankamp, B., Maher, K., Chen, M. H., Tong, S., Tamin, A., Lowe, L., Frace, M., DeRisi, J. L., Chen, Q., Wang, D., Erdman, D. D., Peret, T. C., Burns, C., Ksiazek, T. G., Rollin, P. E., Sanchez, A., Liffick, S., Holloway, B., Limor, J., McCaustland, K., Olsen-Rasmussen, M., Fouchier, R., Gunther, S., Osterhaus, A. D., Drosten, C., Pallansch, M. A., Anderson, L. J., and Bellini, W. J. (2003) Characterization of a novel coronavirus associated with severe acute respiratory syndrome. *Science* **300,** 1394–1399

5. Snijder, E. J., Bredenbeek, P. J., Dobbe, J. C., Thiel, V., Ziebuhr, J., Poon, L. L., Guan, Y., Rozanov, M., Spaan, W. J., and Gorbalenya, A. E. (2003) Unique and conserved features of genome and proteome of SARS-coronavirus, an early split-off from the coronavirus group 2 lineage. *J. Mol. Biol.* **331,** 991–1004

6. Yang, H., Yang, M., Ding, Y., Liu, Y., Lou, Z., Zhou, Z., Sun, L., Mo, L., Ye, S., Pang, H., Gao, G. F., Anand, K., Bartlam, M., Hilgenfeld, R., and Rao, Z. (2003) The crystal structures of severe acute respiratory syndrome virus main protease and its complex with an inhibitor. *Proc. Natl. Acad. Sci. U. S. A.* **100,** 13190–13195

7. Li, W., Moore, M. J., Vasilieva, N., Sui, J., Wong, S. K., Berne, M. A., Somasundaran, M., Sullivan, J. L., Luzuriaga, K., Greenough, T. C., Choe, H., and Farzan, M. (2003) Angiotensin-converting enzyme 2 is a functional receptor for the SARS coronavirus. *Nature* **426,** 450–454

8. Zeng, R., Ruan, H. Q., Jiang, X. S., Zhou, H., Shi, L., Zhang, L., Sheng, Q. H., Tu, Q., Xia, Q. C., and Wu, J. R. (2004) Proteomic analysis of SARS associated coronavirus using two-dimensional liquid chromatography mass spectrometry and one-dimensional sodium dodecyl sulfate-poly-acrylamide gel electrophoresis followed by mass spectrometric analysis. *J. Proteome Res.* **3,** 549–555

9. Zeng, R., Yang, R. F., Shi, M. D., Jiang, M. R., Xie, Y. H., Ruan, H. Q., Jiang, X. S., Shi, L., Zhou, H., Zhang, L., Wu, X. D., Lin, Y., Ji, Y. Y., Xiong, L., Jin, Y., Dai, E. H., Wang, X. Y., Si, B. Y., Wang, J., Wang, H. X., Wang, C. E., Gan, Y. H., Li, Y. C., Cao, J. T., Zuo, J. P., Shan, S. F., Xie, E., Chen, S. H., Jiang, Z. Q., Zhang, X., Wang, Y., Pei, G., Sun, B., and Wu, J. R. (2004) Characterization of the 3a protein of SARS-associated coronavirus in infected vero E6 cells and SARS patients. *J. Mol. Biol.* **341,** 271–279

10. Der, S. D., Zhou, A., Williams, B. R., and Silverman, R. H. (1998) Identification of genes differentially regulated by interferon α, β, or γ using oligonucleotide arrays. *Proc. Natl. Acad. Sci. U. S. A.* **95,** 15623–15628

11. Tonge, R., Shaw, J., Middleton, B., Rowlinson, R., Rayner, S., Young, J., Pognan, F., Hawkins, E., Currie, I., and Davison, M. (2001) Validation and development of fluorescence two-dimensional differential gel electrophoresis proteomics technology. *Proteomics* **1,** 377–396

12. Gharbi, S., Gaffney, P., Yang, A., Zvelebil, M. J., Cramer, R., Waterfield, M. D., and Timms, J. F. (2002) Evaluation of two-dimensional differential gel electrophoresis for proteomic expression analysis of a model breast cancer cell system. *Mol. Cell. Proteomics* **1,** 91–98

13. Gygi, S. P., Rist, B., Gerber, S. A., Turecek, F., Gelb, M. H., and Aebersold, R. (1999) Quantitative analysis of complex protein mixtures using isotope-coded affinity tags. *Nat. Biotechnol.* **17,** 994–999

14. Han, D. K., Eng, J., Zhou, H., and Aebersold, R. (2001) Quantitative profiling of differentiation-induced microsomal proteins using isotope-coded affinity tags and mass spectrometry *Nat. Biotechnol.* **19,** 946–951

15. Patton, W. F., Schulenberg, B., and Steinberg, T. H. (2002) Two-dimensional gel electrophoresis: better than a poke in the ICAT? *Curr. Opin. Biotechnol.* **13,** 321–328

16. Schmidt, F., Donahoe, S., Hagens, K., Mattow, J., Schaible, U. E., Kaufmann, S. H., Aebersold, R., and Jungblut, P. R. (2004) Complementary analysis of the Mycobacterium tuberculosis proteome by two-dimensional electrophoresis and isotope-coded affinity tag technology. *Mol. Cell. Proteomics* **3,** 24–42

17. Yu, L. R., Zeng, R., Shao, X. X., Wang, N., Xu, Y. H., and Xia, Q. C. (2000) Identification of differentially expressed proteins between human hepatoma and normal liver cell lines by two-dimensional electrophoresis and liquid chromatography-ion trap mass spectrometry. *Electrophoresis* **21,** 3058–3068

18. Griffin, T. J., Gygi, S. P., Ideker, T., Rist, B., Eng, J., Hood, L., and Abersold, R. (2002) Complementary profiling of gene expression at the transcriptome and proteome levels in *Saccharomyces cerevisiae. Mol. Cell. Proteomics* **1,** 323–333

19. Kalicharran, K., and Dales, S. (1996) The murine coronavirus as a model of trafficking and assembly of viral proteins in neural tissue. *Trends Microbiol.* **4,** 264–269

20. Li, H. P., Huang, P., Park, S., and Lai, M. M. (1999) Polypyrimidine tract-binding protein binds to the leader RNA of mouse hepatitis virus and serves as a regulator of viral transcription. *J. Virol.* **73,** 772–777

21. Li, H. P., Zhang, X., Duncan, R., Comai, L., and Lai, M. M. (1997) Heterogeneous nuclear ribonucleoprotein A1 binds to the transcription-regulatory region of mouse hepatitis virus RNA. *Proc. Natl. Acad. Sci. U. S. A.* **94,** 9544–9549

22. Zhang, X., Li, H. P., Xue, W., and Lai, M. M. (1999) Formation of a ribonucleoprotein complex of mouse hepatitis virus involving heterogeneous nuclear ribonucleoprotein A1 and transcription-regulatory elements of viral RNA. *Virology* **264,** 115–124

23. Wang, Y., and Zhang, X. (1999) The nucleocapsid protein of coronavirus mouse hepatitis virus interacts with the cellular heterogeneous nuclear ribonucleoprotein A1 *in vitro* and *in vivo. Virology* **265,** 96–109

24. Shen, X., and Masters, P. S., (2001) Evaluation of the role of heterogeneous nuclear ribonucleoprotein A1 as a host factor in murine coronavirus discontinuous transcription and genome replication. *Proc. Natl. Acad. Sci. U. S. A.* **98,** 2717–2722

25. Shi, S. T., Yu, G. Y., and Lai, M. M. (2003) Multiple type A/B heterogeneous nuclear ribonucleoproteins (hnRNPs) can replace hnRNP A1 in mouse hepatitis virus RNA synthesis. *J. Virol.* **77,** 10584–10593

26. Bushell, M., and Sarnow, P. (2002) Hijacking the translation apparatus by RNA viruses. *J. Cell Biol.* **158,** 395–399

27. Kushner, D. B., Lindenbach, B. D., Grdzelishvili, V. Z., Noueiry, A. O., Paul, S. M., and Ahlquist, P. (2003) Systematic, genome-wide identification of host genes affecting replication of a positive-strand RNA virus. *Proc. Natl. Acad. Sci. U. S. A.* **100,** 15764–15769

28. Lai, M. M. (1998) Cellular factors in the transcription and replication of viral RNA genomes: a parallel to DNA-dependent RNA transcription. *Virology* **244,** 1–12

29. Blumenthal, T., and Carmichael, G. G. (1979) RNA replication, function and structure of Qβ-replicase. *Annu. Rev. Biochem.* **48,** 525–548